Title
Cerebral structure on MRI, Part I: Localization of age-related changes

Journal
Biological Psychiatry, 29(1)

ISSN
0006-3223

Authors
Jernigan, Terry L
Archibald, Sarah L
Berhow, Melissa T
et al.

Publication Date
1991

DOI
10.1016/0006-3223(91)90210-d

Peer reviewed

Cerebral Structure on MRI, Part I: Localization of Age-Related Changes

Terry L. Jernigan, Sarah L. Archibald, Melissa T. Berhow, Elizabeth R. Sowell, David S. Foster, and John R. Hesselink

In this report, earlier findings of age-related changes in brain morphology on magnetic resonance (MR) images are extended to include measurements of individual cerebral grey matter structures and an index of white matter degeneration. Volumes of caudate, lenticular, and diencephalic structures are estimated, as are grey matter volumes in eight separate cortical regions. Results suggest that between 30 and 79 years significant decreases occur in the volume of the caudate nucleus, in anterior diencephalic structures, and in the grey matter of most cortical regions. The data suggest that the volumes of the thalamus and the anterior cingulate cortex may be unchanged. Among those cortical regions found to be affected in aging, some evidence is present for greater change in association cortices and mesial temporal lobe structures. There are also dramatic age-related changes in the white matter, manifest as lengthened T_2 values on MR images.

Introduction

Age-related changes in morphological characteristics of the brain in nondemented elderly have been amply documented by neuropathological investigations (Dekaban and Sadowsky 1978; Ho et al 1980; Davis and Wright 1977; Hubbard and Anderson 1981; Critchley 1942; Brody 1955, 1973, 1978; Bugiani et al 1978; Henderson et al 1980). Most of these studies have focused on decreases in brain weight or volume, or decreases in volume or cell density of the cerebral cortex. No systematic studies of age-related changes in individual subcortical grey matter structures are available, and in most studies of the cortex, only a few cortical regions have been measured concurrently. Magnetic resonance imaging (MRI) of the brain is the first in vivo method with sufficient resolution to permit investigations of gross structural variation in living subjects. An earlier report (Jernigan et al 1990) described semi-automated morphometric techniques and several age-related morphological changes detected with these methods. Linear increases in the volume of ventricular and cortical sulcal cerebrospinal fluid (CSF) were accompanied by a substantial reduction in cortical grey matter with advancing age. Quantitative measures of signal hyperintensities within the white matter were also applied in the previous study. These measures revealed significant increases in these abnormalities in the elderly subjects,

From the VA Medical Center (TLJ) and the Brain Image Analysis Laboratory (SLA, MTB, ERS, DSF) and Departments of Psychiatry (TLJ), Radiology (TLJ, JRH), and the Neurosciences (JRH), University of California, San Diego, CA.
Address reprint requests to University of California, San Diego, Terry L. Jernigan, Ph.D., Department of Psychiatry, 0631, 9500 Gilman Drive, La Jolla, CA 92093-0631.
Received April 26, 1990; revised July 5, 1990.

Published 1991 by Elsevier Science Publishing Company, Inc.
ISSN/91/$0.00

a finding noted in qualitative evaluations of normal elderly subjects by several investigators (Gerard and Weisberg 1986; Awad et al 1986a, 1986b, 1987; Fazekas et al 1987; Kertesz et al 1988). The present study further describes the age-related changes in brain structure, focusing on specific cerebral grey matter structures, both cortical and subcortical, in adults between 30 and 79 years of age. In addition, a recently developed index of altered signal strength in the cerebral white matter has been applied.

Materials and Methods

Subjects

Fifty-five normal volunteers (21 women, 34 men) were recruited and screened for any evidence of significant medical, neurological, psychiatric, or intellectual disorder. They ranged in age from 30 to 79 years (53.8 ± 14.1 mean ± SD), and had completed between 11 and 22 years of education (14.8 ± 2.7). Forty-nine of the subjects were also subjects in the earlier study.

Imaging Protocol

Magnetic resonance (MR) was performed with a 1.5-T superconducting magnet (Signa; General Electric, Milwaukee) at the UCSD/AMI Magnetic Resonance Institute. Proton-density weighted (PDW) and T_2-weighted (T_2W) images (Figure 1) were obtained simultaneously for each section, using an asymmetrical, multiple-echo sequence (TR = 2000 msec, TE = 25, 70 msec) to obtain images of the entire brain in the axial plane. Section thickness was 5 mm with a 2.5-mm gap between successive sections in all instances. A 256 × 256 matrix and 24-cm field of view were used. All subjects were unsedated for the examination. For the following discussion of image analysis, the term pixel will be used to refer to a single picture element (or signal value) from the image matrix. The term voxel will be used to refer to the corresponding three-dimensional volume from which the signal value for a pixel arises.

Image Analysis

The visual identification of specific structures in MR images is possible because of the tissue contrast between the grey matter structures and the surrounding white matter or CSF. However, measurements of volumes of cerebral structures must overcome several problems. First, because of partial-voluming of grey matter with white matter or CSF (or both) at the edges of structures, sharply defined edges are not always present. This allows considerable scope for variability in subjective determinations of such boundaries when, for example, tracing methods are used, leading to measurement unreliability in the computed volumes.

Visual determination of specific cortical structures on MRI presents additional challenges and depends upon the presence of visible gross morphological features relative to which the boundaries of the cortical regions can be defined. Standard regional divisions for the cortex are based to a large extent on cortical gyral patterns, but the accurate localization of particular gyri or sulci, throughout a series of images, is often impossible. Furthermore, some boundaries, such as that between posterior temporal and inferior parietal cortex, are not clearly defined in gross morphological terms. Also, even when

attempts are made to standardize head positioning, rotation of the head (relative to the imaging plane) occurs in all three planes. This is especially true with unsedated subjects who must be sufficiently comfortable in position to avoid movement during the imaging session. Careful inspection indicates that relatively small rotations substantially change the appearance of brain structures in the image plane, further complicating their visual identification. Thus, manually tracing the structures in the sections where they are best visualized often leads to inaccurate volume and asymmetry assessments. The techniques described below are designed to address these difficulties.

To facilitate and standardize the determination of structural edges, our method involves a semiautomated classification of all pixels in the images on the basis of their signal characteristics on the two original images of each section. A detailed description of the basic image analysis method has been previously reported (Jernigan et al 1990). Only a brief summary is provided here: For each axial brain section imaged, a computed matrix is produced. In this matrix, voxels are classified as most resembling (in signal strength) grey matter, white matter, CSF, or signal hyperintensities (tissue abnormalities). The procedure involves first isolating intracranial areas and discarding other pixels from the images, then applying a high-pass digital filter to reduce artifactual signal drift due to field inhomogeneities. Next, the two image matrices (PDW and T_2W) are combined using an empirically derived linear combination to separate CSF from brain. CSF is classified by applying a classification criterion to these new matrix values. The PDW and T_2W matrices are then combined using another linear combination to separate grey matter from white matter. Classification of remaining pixels is done by applying a criterion to these new values. A pixel is classified as a signal hyperintensity if the signal values on both PDW and T_2W images are above the range of all other tissues. The full series of axial images is analyzed, beginning at the bottom of the cerebellar hemispheres and extending through the vertex.

As discussed in the earlier report, the pixel-classification method has several limitations. One is that the classification criteria must be calibrated by reference to sampled values from within the brain. Thus, changes in tissue values may lead to inappropriate adjustment of the criteria. Preliminary results suggest that this factor contributes little variability to the grey matter classification, however. Because of overlapping signal distributions of grey matter pixels and those in mild or partially volumed signal hyperintensities, the classification of hyperintense areas is quite conservative. For this reason, an attempt has been made (described below) to measure areas within white matter that have moderately elevated T_2. Further manipulations to derive the specific structural measures for the present study were made using these "pixel-classified" images. Trained operators, blind to any subject characteristics, used a stylus-controlled cursor on the displayed images to manually separate cerebellar from cerebral areas, left from right hemispheres, and the cortical from subcortical regions. Thus, separate estimates of the four classes of pixels were made for these areas.

Definition of Subcortical Structures

To delineate subcortical structures, the operators circumscribed pixels classified as grey matter that were visually determined to be in caudate nuclei, lenticular nuclei, and diencephalic grey matter structures (including mammillary bodies, hypothalamic grey, septal nuclei, and thalamus). They did not trace the edges of the structures, but defined polygons that included all grey matter pixels within the structures, and excluded those

grey matter pixels associated with other structures. In some cases, when the subcortical nuclei were contiguous with other areas classified as grey but clearly not in the structures, boundaries were manually constructed using the filmed images as a guide. Estimates of the volumes of the subcortical structures were made by summing the designated grey matter pixels across all sections.

Definition of Cortical Regions

To define anatomically consistent cortical regions, a method was adopted for making subdivisions of the cerebrum relative to the centromedial structural midline and two consistently identifiable points: the most anterior midline point in the genu and the most posterior midline point in the splenium of the corpus callosum. By calculating rotation angles using these landmarks, it was possible to perform a three-dimensional rotation of the images, thus correcting each individual's image data for rotation out of the optimal imaging plane. Regions could then be constructed that resulted in highly consistent placement of regional boundaries relative to gross anatomic landmarks.

The orientation of the midsagittal plane was first determined by computing a regression line through a series of visually selected brainstem midline points. The division of the cerebrum was then based on two major planes (Figure 2)—an *axial plane*, which is perpendicular in orientation to the midsagittal plane and passes through the two corpus callosum points, and a *coronal plane*, which is defined as perpendicular to the first plane and which passes through the midpoint between the two corpus callosum points. By computing new coordinates for each voxel relative to these planes, each is assigned to one of four zones: (1) inferior to the axial plane and anterior to the coronal plane (IA); (2) inferior to the axial plane and posterior to the coronal plane (IP); (3) superior to the axial plane and anterior to the coronal plane (SA); and (4) superior to the axial plane and posterior to the coronal plane (SP). Again, these defined planes are independent of the image plane, as a three-dimensional rotation is first applied based on the positions of the landmarks described above. Anterior temporal, orbitofrontal, and some dorsolateral and mesial frontal cortex lies in the inferior anterior zone. Posterior temporal and inferior occipital cortex falls in the inferior posterior zone. Most of the remaining parts of the frontal lobe fall into the superior anterior zone, and the superior posterior zone contains primarily parietal and a small portion of the superior occipital cortex.

To further separate mesial from peripheral cortical regions, an ellipsoid volume was defined within the supratentorial cranial vault. This volume constitutes 30% of the supratentorial volume and has cardinal dimensions proportional to those of the supratentorial vault (i.e., the z-axis extent of the ellipsoid is proportional to the maximum z-axis extent of the supratentorial cranium, the y-axis extent of the ellipsoid to the maximum y-axis extent, and the x-axis to the maximum x-axis extent). The ellipsoid is centered slightly behind, but in the same axial plane as, the origin of the coordinate system described above, at a point 60% of the distance from the genu to the splenium reference point along the line connecting them. The size and center point of the volume were chosen empirically so as to isolate as well as possible the medial cortical surfaces of the limbic lobe (Broca 1878), while excluding the more lateral neocortical surfaces. The area designated as mesial with this method is shown in green in Figure 3. It consistently includes the most posterior parts of the orbital frontal lobe (including the anterior perforated substance and related basal forebrain structures), the amygdala, the hippocampus and most of the parahippocampal gyrus, the insula, and most of the cingulate gyrus. The ellipsoid defines

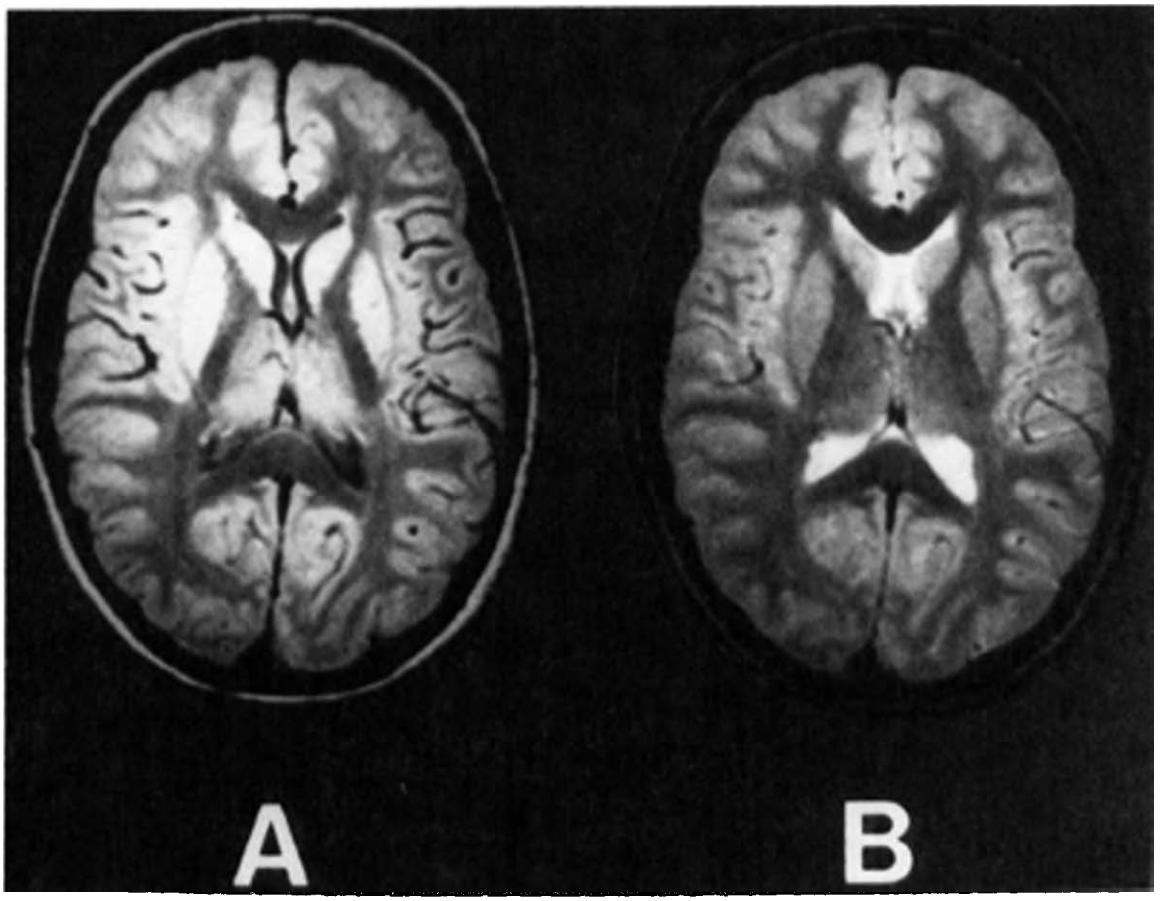

Figure 1. Representative images from the standard protocol. (A) Axial section, SE 2000/25 (PDW in text). (B) Axial section, SE 2000/70 (T_2W in text). Sections are 5 mm thick, matrix 256 × 256, with 2.5-mm gaps between images. A field of view of 24 cm was used.

mesial and peripheral zones within each of the four original cerebral zones defined above. A summary of the cortical structures falling into each of the resulting eight zones is given in Table 1.

The fully processed images are illustrated in Figure 3. The different pixel classes are color coded as follows: Diencephalic areas are blue, caudate nuclei are magenta, and lenticular nuclei are orange. Within the subcortical white matter there are some voxels with signal values that fall not within the criterion range for white, but within the range of grey matter values (i.e., they demonstrate lengthened T_2 relative to other white matter voxels). These voxels have been coded separately and are shown in Figure 3 in yellow. The blue line running through each section indicates the position of the coronal dividing plane. Because this plane passes through the diencephalic grey matter regions and divides the functionally distinct anterior hypothalamic and septal structures (lying anteriorly) from the bulk of the thalamus (lying posteriorly), the corresponding anterior and posterior diencephalic areas were examined separately. It should be noted that areas within the lenticular nucleus containing significant iron deposits, particularly in globus pallidus, do not meet the signal criteria for grey matter and are thus not included in this region. Fluid and white matter are shown in red and black, respectively; however, subcortical and cortical fluid are measured separately.

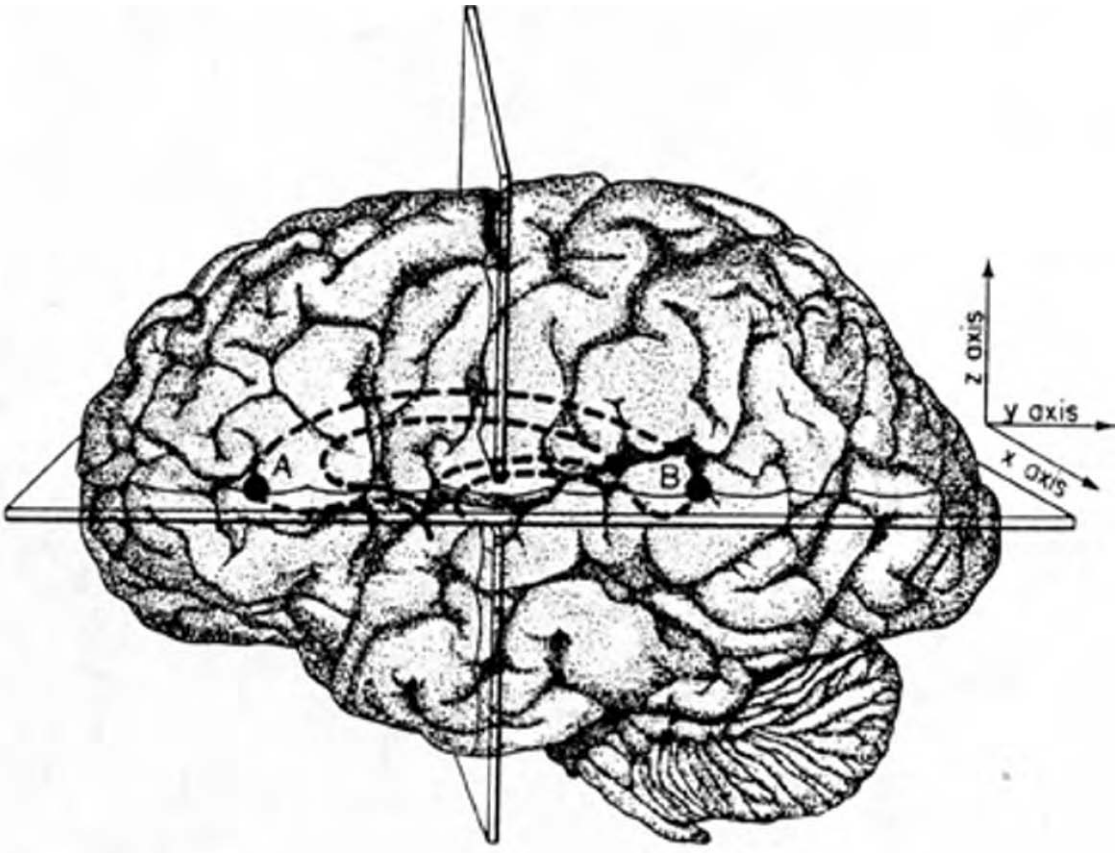

Figure 2. Cerebral regions are defined as follows: Points A and B in the corpus callosum, shown above, are the most anterior midline point in the genu, and the most posterior midline point in the splenium, respectively. An axial plane passing through these two points is defined, as shown, perpendicular to the midsagittal plane. A coronal plane is defined perpendicular to the axial plane and passing through the midpoint between points A and B. Thus four cerebral zones are defined: inferior anterior, inferior posterior, superior anterior, and superior posterior. Anterior temporal, orbitofrontal, and some dorsolateral and mesial frontal cortex lies in the inferior anterior zone. Posterior temporal and inferior occipital cortex falls in the inferior posterior zone. Most of the remaining parts of the frontal lobe fall into the superior anterior zone, and the superior posterior zone contains primarily parietal and superior occipital cortex.

Volume of the supratentorial cranium was estimated by summing supratentorial voxels (including CSF, hyperintensities, and grey and white matter) over all sections. The grey matter voxels within each of the subcortical structures and the cortical grey matter voxels within each of the eight cerebral zones were summed separately. Eight regional volumes were also computed by summing all supratentorial voxels (including CSF, hyperintensities, and grey and white matter) within each region. Those diencephalic structures falling within the anterior cerebral zone (i.e., before the defined *coronal* plane), including septal nuclei, anterior hypothalamic grey, and some basal forebrain regions (Figure 3), constitute a separate measure from the measure of the posterior diencephalon which consists almost entirely of thalamus. In addition to these grey matter volumes, the total volume of the subcortical white matter was estimated by summing all such voxels whether or not they had normal signal intensity. Finally, an index of signal alterations in the white matter was constructed by summing voxels within the subcortical white matter regions having

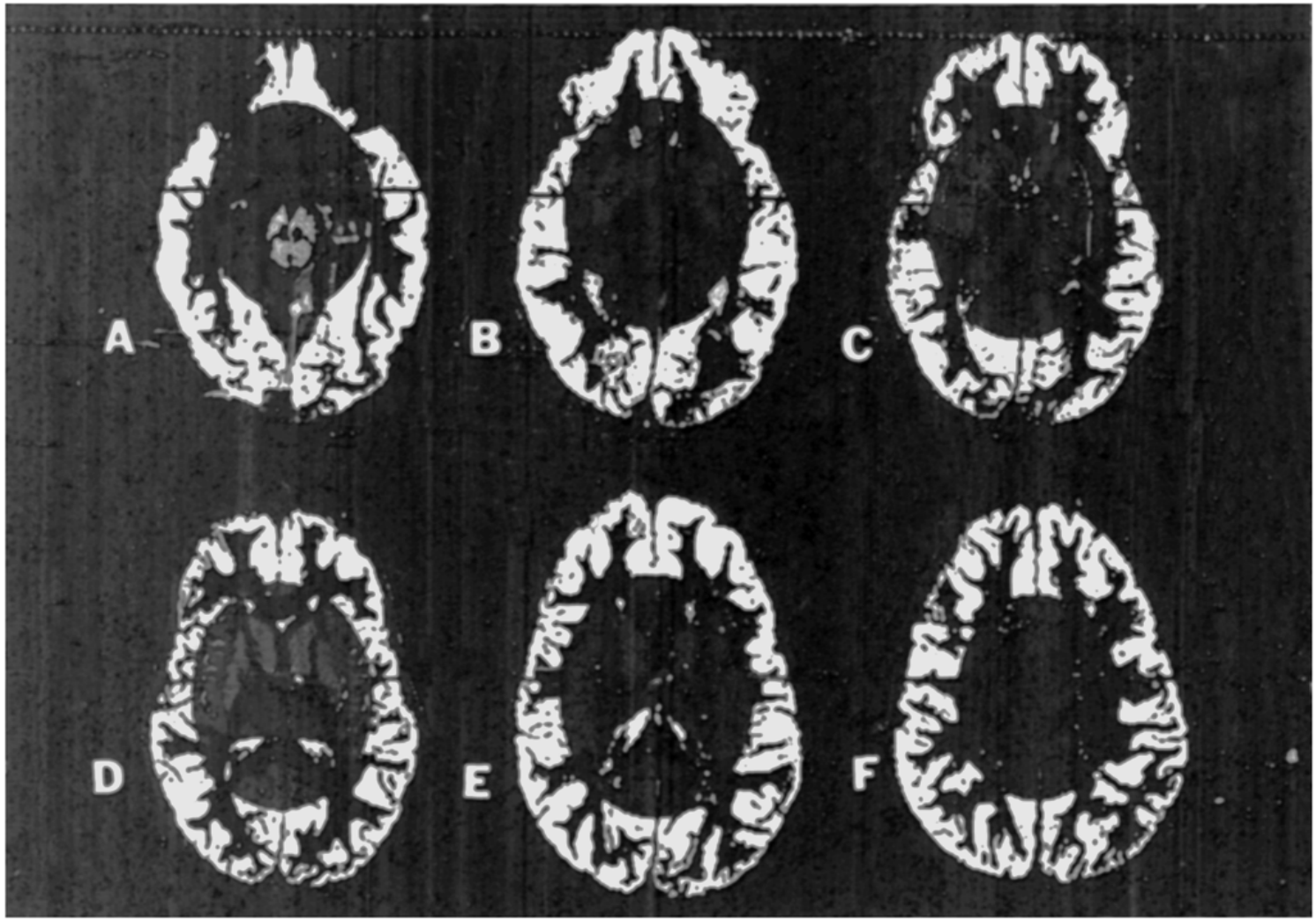

Figure 3. Representative, fully processed images. Pixels are classified and zones have been manually designated. The grey matter pixels have been color-coded to display the zone designations: peripheral cortex = white, mesial cortex = green, caudate = pink, lenticular nucleus = orange, diencephalon = blue, and cerebellar = grey. CSF and white matter pixels in all zones are displayed here in red and black, respectively; however, these pixels are coded separately by zone so that regional measures may be computed. The yellow pixels within the subcortical zone are white matter having the signal characteristics of grey matter. Sections completely classified as (A–C) inferior to dividing plane and as (D–F) superior to dividing plane; for both sections the blue line within shows the position of the coronal dividing plane. The ellipsoid defining the mesial cortex has cardinal dimensions proportional to those of the supratentorial cranium and occupies 30% of its volume.

Table 1. Summary of Cortical Structures Within Each Cerebral Region

Peripheral cortex
Inferior anterior
Frontal cortex including most of the orbitofrontal cortex and the inferior mesial frontal cortex (excluding most of the cingulate)
The cortex of the temporal pole (excluding the uncus)
Inferior posterior
Most of the lateral surface of the temporal lobe (excluding the temporal pole)
The inferior occipital lobe
Superior anterior
Frontal cortex including most of the dorsolateral frontal cortex and the superior mesial frontal cortex (excluding most of the cingulate)
The frontal operculum
Superior posterior
Most of the parietal lobe
The superior occipital lobe
Mesial cortex
Inferior anterior
The mesial parts of the orbitofrontal cortex
Most of the inferior cingulate
The anterior insula below the frontal operculum
The uncus and part of the amygdala
Inferior posterior
Part of the amygdala
The hippocampal formation and parahippocampal gyrus
The posterior insula below the parietal operculum
Superior anterior
Anterior insula at the level of the frontal operculum
Anterior cingulate above the genu of the corpus callosum
Superior posterior
Posterior insula at the level of the parietal operculum
Posterior cingulate above the splenium of the corpus callosum

signal characteristics meeting criteria for "grey matter" or for "signal hyperintensities," i.e., they had longer T_2 values than is normal for white matter. All subcortical measures were expressed as proportions of the supratentorial cranial volume, and all cortical measures as proportions of their respective regional volumes.

Statistical Analysis

The magnitude and significance of age-related changes were estimated with Pearson product–moment correlation coefficients. Previous studies (Zatz et al 1982; Pfefferbaum et al 1986) have suggested that some age-related changes in brain structure are not linear over the adult age range, but show accelerated change in the elderly. For this reason, polynomial regressions were performed to detect significant deviations from linearity. If the simple correlation (linear component) of age with a morphological measure was statistically significant, a quadratic term (age-squared) was added to the regression of age on the measure. If the addition of this variable significantly increased R^2, the function was considered to be nonlinear, and the function with both terms is given here. Similarly, if a cubic term further (significantly) increased R^2, then a function with all three terms is given.

Table 2. Correlations of Cerebral Grey Proportions and White Matter Measures With Age

	r	p
Overall subcortical grey	−0.38	0.004
Caudate	−0.49	0.000
Lenticular	−0.24	0.082
Diencephalic	−0.07	0.614
Anterior	−0.34	0.012
Posterior	0.11	0.425
Overall cortical grey	−0.45	0.001
Peripheral cortex		
Inferior anterior	−0.40	0.002
Inferior posterior	−0.37	0.006
Superior anterior	−0.38	0.004
Superior posterior	−0.37	0.005
Mesial cortex		
Inferior anterior	−0.32	0.016
Inferior posterior	−0.44	0.001
Superior anterior	−0.13	0.329
Superior posterior	−0.31	0.022
White matter volume	−0.04	0.788
White matter index	0.68[a]	0.000

[a]Multiple *R* with linear and quadratic terms.

Results

Clinical evaluation of the images yielded no focal abnormalities indicative of masses or infarction; however, images from several elderly subjects showed multiple areas of signal hyperintensity within the white matter. In one 59-year-old woman, a right cerebellar venous angioma was noted.

For the subcortical grey matter measures, in no case did the quadratic term significantly improve a simple linear correlation; however, for the caudate nucleus it closely approached significance ($p < 0.06$). Also, although the linear correlation of the lenticular measure with age did not reach significance, it should be mentioned that the quadratic term significantly improved this nonsignificant correlation from $r = 0.24$ ($p < 0.09$) to multiple $r = 0.39$ ($p < 0.02$). There was no evidence for nonlinearity in the age functions for the cortical grey matter measures, as no quadratic term even approached significance.

There was no evidence for a reduction of overall white matter volume ($r = -0.04$, $p = 0.79$). For the measure of white matter signal abnormalities, however, the linear age term was highly significant and the quadratic term significantly improved the fit. The correlations with age of the subcortical structural volumes (expressed as proportions of the cranium), the regional cortical grey matter volumes (expressed as proportions of their respective regions), and the white matter measures are provided in Table 2. It should be noted that post hoc analyses of gender effects revealed no significant differences for 16 of the 17 measures, a result consistent with chance.

Overall, subcortical grey matter significantly declines with age. The most pronounced loss appears to occur in caudate nuclei. A scatterplot of caudate proportions across the age range is provided in Figure 4. No significant linear reduction with age is observed in the lenticular measure, though, as noted above, there is some indication that a nonlinear decrease may be present. The overall diencephalic measure shows no suggestion of

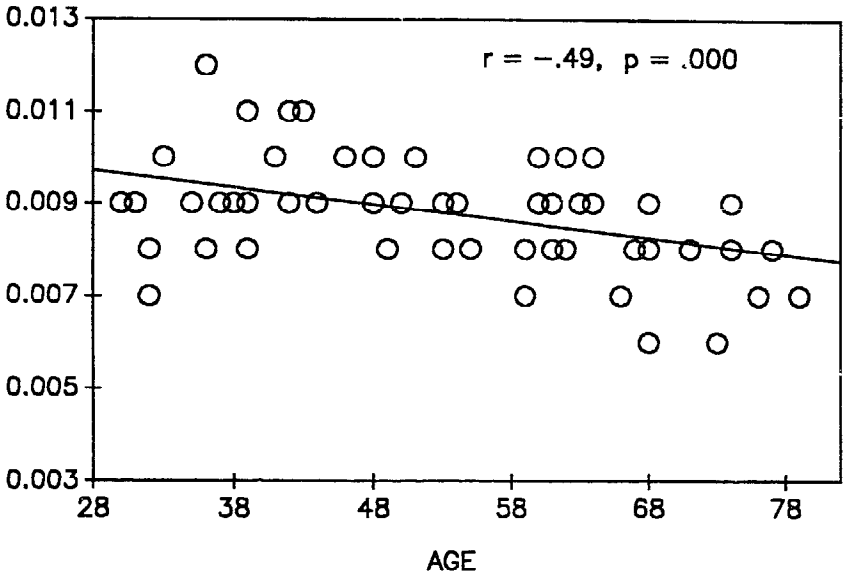

Figure 4. Scatterplot of values for the volume of the caudate nuclei, expressed as a proportion of the supratentorial cranium, across the age range of the subjects.

significant decrease; however, there appears to be selective loss in the anterior diencephalic structures.

Within the cortex, all regions with the exception of mesial SA show significant decreases. Although the magnitude of decline is similar across the peripheral regions, there is some indication that among mesial cortices, the IP zone (mostly mesial temporal) shows a larger reduction. In fact, among the mesial cortical measures, only this one significantly improves the statistical prediction of age based on the volume of peripheral cortices alone (Table 3). The decrease in the mesial IP proportion is shown graphically in Figure 5.

The white matter index shows a highly significant, nonlinear increase with advancing age (Figure 6), suggesting diffuse alterations of white matter signal values. It should be noted that the quadratic component is probably due to the acceleration in the age-related increase after the age of 60. A monotonic function is probably more plausible; however, further polynomial terms (which may have produced a more plausible function) failed to reach significance.

Discussion

These results provide a description of the regional pattern of cerebral grey matter losses occurring across the age range in normal volunteers. As always, it is possible that the discrepancies observed between different regions are due either to chance, or to differences

Table 3. Multiple Regression of Peripheral and Mesial IP Cortical Grey Measures on Age

Variable	Regression coefficient	t	p (two tailed)
Total peripheral cortex	−0.26	−1.79	0.08
Mesial IP cortex	−0.29	−2.02	0.05
Overall regression: Multiple $r = 0.49$, $F = 8.25$, $p < 0.001$.			

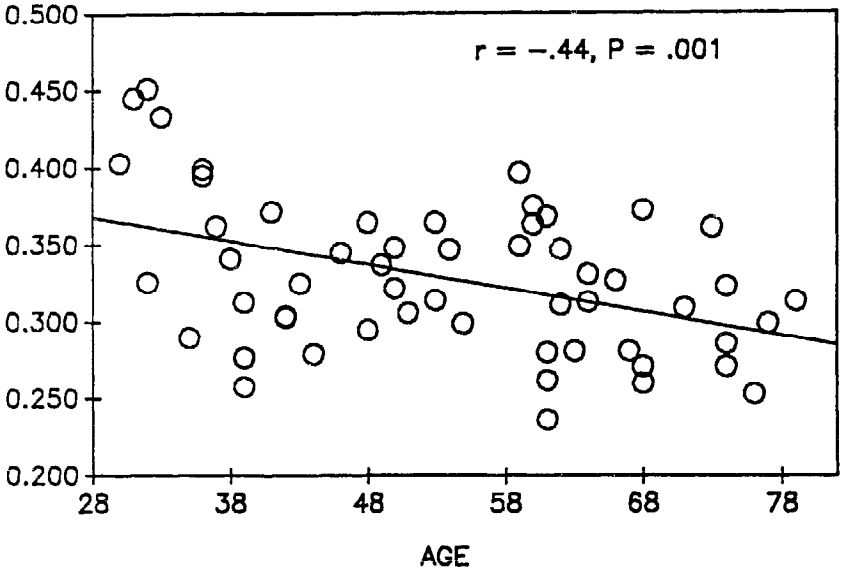

Figure 5. Scatterplot of values for the volume of mesial IP cortical grey, expressed as a proportion of the total volume of this regional zone, across the age range of the subjects. This region includes posterior insular cortex, mesial temporal lobe structures, and some retrosplenial cortex of the limbic lobe.

in measurement sensitivity (i.e., measures with less sensitivity will yield smaller effects even if the underlying effects are equal in size). It is unlikely, however, that a discrepancy such as that between the thalamus and the caudate is due to measurement sensitivity, since the thalamus is a relatively large, regularly shaped structure that is well-delineated

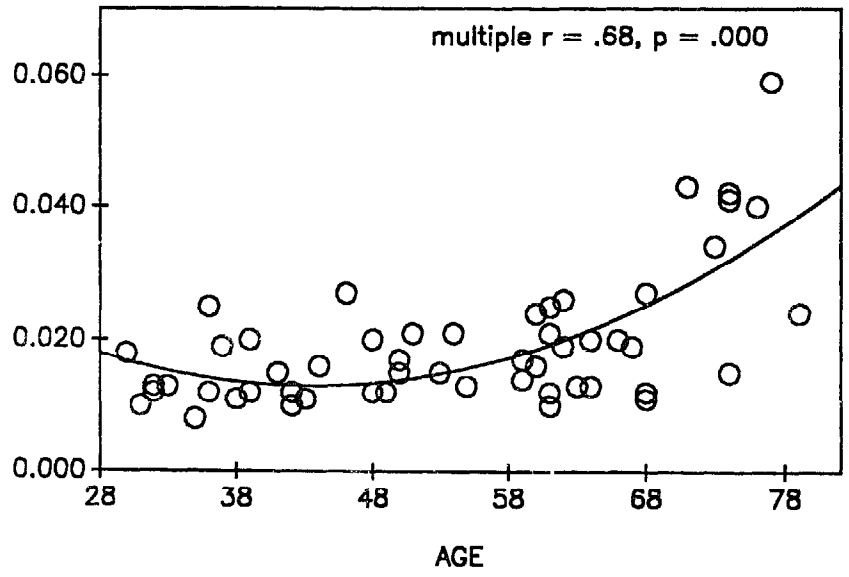

Figure 6. Scatterplot of values on the index of white matter abnormality across the age range of the subjects. The increase has a significant quadratic component.

by the internal capsule. Thus those factors such as unreliability of boundary determination and inaccuracy due to between-section gaps, which reduce measurement sensitivity, would have less impact on this measure than on the measure of the smaller, less regularly shaped caudate and the even smaller anterior diencephalic structures. Unfortunately, the measure of the lenticular nucleus may have suffered from inaccuracy due to variations in iron deposition. Such accumulations, most concentrated in the globus pallidus, significantly reduce the signal values in this structure on T_2-weighted images (Drayer 1988; Drayer et al 1986). Thus many voxels within the grey matter of the globus pallidus may not meet our signal criteria for grey matter. The age-related decline in the lenticular nucleus may therefore be greater than we estimate, or the trend observed here may be due to age-related accumulation of iron in the structure, rather than a true volume reduction. Even considering these factors, it seems likely that significant reduction of the caudate nucleus and anterior diencephalic structures occurs in aging, and that changes in the thalamus are much smaller, if they exist at all. The decrease in the caudate is consistent with data from neuropathology studies (Bugiani et al 1978) and may be relevant to age-related changes in dopaminergic activity (McGeer 1981; McGeer and McGeer 1976). Finch (1980) has discussed the possible relation of age-related losses in the striatum to the onset of Huntington's chorea. As these age-related changes appear to be measurable in vivo, it may be possible to test such hypotheses directly.

The anterior diencephalic region consists of a group of small structures, including anterior hypothalamic grey nuclei, septal nuclei, and basal forebrain nuclei. As several of these areas are strongly cholinergic, and central cholinergic activity has been implicated in memory function and Alzheimer's disease (Drachman and Leavitt 1974; Coyle et al 1983), the changes observed here are of particular interest. The volume reductions may be accompanied by reduced cholinergic innervation of the cortex with significant implications for cognitive decline in old age.

The cortical changes appear to be more evenly distributed, especially among the peripheral cortices. These areas contain most of the association areas of the neocortex. Of the mesial cortices, the IP region, which consists largely of posterior insula, hippocampus, and parahippocampal gyrus, may be particularly decreased in aging. The results of the regression analysis summarized in Table 3 suggest that age-related changes in this region are to some extent independent of those in the peripheral cortices. Because the significance of a regression coefficient in such analyses reflects the *unique* predictive power of a measure, the fact that both cortical measures have regression coefficients approaching significance means that they are unlikely to be measuring the same diffuse process. Separate processes occurring in aging may contribute differently to the changes in these two regions.

Henderson et al (1980) made cell counts in several cortical regions and demonstrated decreases over the adult age range, especially in "large neuron" populations. In that study, as in this one, a large degree of variability among individuals of all ages was observed. The variability and magnitude of decline observed with their methods are consistent with the functions given here. For example, the age correlation for their superior temporal lobe sample of "small neurons" was -0.396 ($p < 0.01$), and for the combined temporal lobe samples of "large neurons" was -0.445 ($p < 0.001$) over the age range from 20 to 95 years. Over a more restricted age range (30–79 years), we observe similar reductions in cortical volumes. In the IP region (temporal and occipital lobes), the peripheral cortex correlation is -0.37 ($p < 0.006$), and the mesial cortex correlation is -0.44 ($p < 0.001$). Thus, although these data are obviously not directly comparable, there is the

suggestion that the two methods may be measuring closely associated cerebral changes occurring during this age range.

The lack of age-related change in the volume of subcortical white matter implies that the previously reported age increases in CSF are associated with reductions in grey matter volume. This does not mean, however, that the grey matter structures are affected with no consequence to their associated fiber tracts, but only that such consequences may be manifested as signal changes within the white matter rather than shrinkage. These observed signal changes in the white matter agree with earlier reports of an increasing incidence of visually identified high signal areas in the elderly (Gerard and Weisberg 1986; Awad et al 1986a, 1986b, 1987; Fazekas et al 1987; Kertesz et al 1988). The age function reported here for the index of white matter abnormality is quite similar to that obtained with our measure of subcortical hyperintensities (Jernigan et al 1990). It was our impression, however, that diffuse pallor in deep white matter on MR images, represented by our methods as voxels with signal characteristics of grey matter, might precede the focal, frankly hyperintense areas noted clinically. Our results do suggest that these areas of mild signal elevation increase with aging, and that the volume of such areas is highly correlated with the volume of subcortical hyperintensities, i.e., areas with T_2 values well above grey matter. This correlation in the present sample is 0.73 ($p < 0.001$). Although this mild, diffuse signal change appears to be strongly related to the hyperintensities, it is less evident upon clinical inspection. Assessment of this subtler change may provide a more sensitive measure of white matter change in patients with few frank hyperintensities, but the present study provides little evidence for this contention.

In summary, a large degree of normal variability is observed in these structural volume measures. Such wide variability has also been observed in neuropathological studies (Hubbard and Anderson 1981; Brody 1978; Henderson et al 1980). When structural volumes vary substantially, even moderately large reductions may not be detectable in individual subjects. However, the group results reported here confirm that volume reductions in specific cortical and subcortical cerebral structures, and changes in the composition, but not the volume, of cerebral white matter, occur across the age range in normal subjects, and demonstrate that these changes may be measured in vivo with morphometric techniques. It is hoped that this information will provide a more accurate context into which the changes associated with pathological aging may be placed. The results also raise questions about the significance of these changes for the functional variability observed among the nonsymptomatic elderly. Preliminary correlative studies to address some of these questions with neuropsychological evaluations of the subjects are currently underway.

This investigation was supported by funds from the Medical Research Service of the Veterans Administration to Terry Jernigan, Ph.D. We especially thank Neison Butters, Ph.D., Chief, Psychology Service, San Diego VA Medical Center for his helpful suggestions.

References

Awad IA, Spetzler RF, Hodak JA, Awad CA, Carey R (1986a): Incidental subcortical lesions identified on magnetic resonance imaging in the elderly. I. Correlation with age and cerebrovascular risk factors. *Stroke* 17:1084–1089.

Awad IA, Johnson PC, Spetzler RF, Hodak JA (1986b): Incidental subcortical lesions identified on magnetic resonance imaging in the elderly. II. Postmortem pathological correlations. *Stroke* 17:1090–1097.

Awad IA, Spetzler RF, Hodak JA, Awad CA, Williams F Jr, Carey R (1987): Incidental lesions noted on magnetic resonance imaging of the brain: Prevalence and clinical significance in various age groups. *Neurosurgery* 20:222–227.

Broca P (1878): Sur la préparation des hémisphères cérébraux. *Rev Anthropol* 7:385–498.

Brody H (1955): Organization of the cerebral cortex. II. A study of aging in the human cerebral cortex. *J Comp Neurol* 102:511–556.

Brody H (1973): Aging of the vertebrate brain. In Rockstein M (ed), *Development and Aging in the Nervous System*. New York: Academic, pp 121–134.

Brody H (1978): Cell counts in cerebral cortex and brainstem. In Katzman R, Terry RD, Bick KL (eds), *Alzheimer's Disease: Senile Dementia and Related Disorders (Aging, Vol. 7)*. New York: Raven, pp 345–351.

Bugiani O, Salvarani S, Perdelli F, Mancardi GL, Leonardi A (1978): Nerve cell loss with aging in the putamen. *Eur Neurol* 17:286–291.

Coyle JT, Price DL, DeLong MR (1983): Alzheimer's disease: A disorder of cortical cholinergic innervation. *Science* 219:1184–1190.

Critchley M (1942): Ageing of the nervous system. In Cowdry EV (ed), *Problems of Ageing*. Baltimore: Williams & Wilkins, pp 518–534.

Davis PJM, Wright EA (1977): A new method for measuring cranial cavity volume and its application to the assessment of cerebral atrophy at autopsy. *Neuropathol Appl Neurobiol* 3:341–358.

Dekaban AS, Sadowsky D (1978): Changes in brain weights during the span of human life: Relation of brain weights to body heights and body weights. *Ann Neurol* 4:345–356.

Drachman DA, Leavitt J (1974): Human memory and the cholinergic system: A relationship to aging? *Arch Neurol* 30:113–121.

Drayer BP (1988): Imaging of the aging brain. Part I. Normal findings. *Radiology* 166:785–796.

Drayer B, Burger P, Darwin R, Riederer S, Herfkens R, Johnson GA (1986): MRI of brain iron. *Am J Roentgenol* 147:103–110.

Fazekas F, Chawluk JB, Alavi A, Hurtig HI, Zimmerman RA (1987): MR signal abnormalities at 1.5 T in Alzheimer's dementia and normal aging. *Am J Roentgenol* 149:351–356.

Finch CE (1980): The relationships of aging changes in the basal ganglia to manifestations of Huntington's chorea. *Ann Neurol* 7:406–411.

Gerard G, Weisberg LA (1986): MRI periventricular lesions in adults. *Neurology* 36:998–1001.

Henderson G, Tomlinson BE, Gibson PH (1980): Cell counts in human cerebral cortex in normal adults throughout life using an image analysing computer. *J Neurol Sci* 46:113–136.

Ho K, Roessmann U, Straumfjord JV, Monroe G (1980): Analysis of brain weight. 1. Adult brain weight in relation to sex, race, and age. *Arch Pathol Lab Med* 104:635–639.

Hubbard BM, Anderson JM (1981): A quantitative study of cerebral atrophy in old age and senile dementia. *J Neurol Sci* 50:135–145.

Jernigan TL, Press GA, Hesselink JR (1990): Methods for measuring brain morphologic features on magnetic resonance images: Validation and normal aging. *Arch Neurol* 47:27–32.

Kertesz A, Black SE, Tokar G, Benke T, Carr T, Nicholson L (1988): Periventricular and subcortical hyperintensities on magnetic resonance imaging. *Arch Neurol* 45:404–408.

McGeer EG (1981): Neurotransmitter systems in aging and senile dementia. *Prog Neuropsychopharmacol* 5:435–445.

McGeer EG, McGeer PL (1976): Neurotransmitter metabolism in the aging brain. In Terry RD, Gershon S (eds), *Neurobiology of Aging, Vol 3*. New York: Raven, pp 389–403.

Pfefferbaum A, Zatz LM, Jernigan TL (1986): Computer-interactive method for quantifying cerebrospinal fluid and tissue in brain CT scans: Effects of aging. *J Comput Assist Tomogr* 10:571–578.

Zatz LM, Jernigan TL, Ahumada AJ (1982): Changes on computed cranial tomography with aging: Intracranial fluid volume. *Am J Neuroradiol* 3:1–11.